

Analysis of Surface Morphology of CdTe Thin Film Using Digital Image Processing

Suha H. Ibraheem

College of Basic Education

Mustansiriyah University

Baghdad, IRAQ

ABSTRACT

This study aims to analyze the scanning electron microscope (SEM) images of cadmium telluride (CdTe) thin films. Image processing techniques were applied to the SEM images to measure the effect of film thickness and annealing process on the porosity, average and pore radius deviation distribution of the film. In addition, edge detection technique was used to identify grain boundaries.

Keywords: CdTe thin films, SEM images, Surface Morphology, Porosity, Grain boundary.

1. INTRODUCTION

II-VI semiconductor thin films are now used in a variety of electronic devices, from solar cells to field-effect transistors, detectors, photodiodes, and photoconductors [1]. Among these materials, cadmium telluride (CdTe) stands out as a key semiconductor in this field, as it has a direct energy gap of about 1.5 eV at 300 K, which enables it to absorb sunlight very efficiently. The optical absorption coefficient of this compound is also very high, registering a value exceeding 10^4 cm^{-1} , which means that it can exploit light more efficiently than the optical absorption limit[2].

Among the different techniques for producing CdTe thin films, thermal evaporation is the only technique that produces contradictory results compared to other techniques, as is known from previous work. By changing the deposition parameters, intrinsic p-type and n-type semiconductors of CdTe can be deposited using this technique[3].

2. DIGITAL IMAGE PROCESSING

The advent of cheap microcomputers and digital cameras with high processing power, image digitizers and processing cards led to further developments in image processing and its applications. Digital image processing can be successfully applied to different types of micrographs and can be combined with other characterization methods such as microtopography or lifetime measurements [4]. The interest in applying image processing in surface science seems clear. Depending on the scale, the goal is always a direct or indirect visual assessment of the surface structure. This also applies to micro and nano science and technology. For some materials, it can be really difficult to visualize grains using conventional grain size analysis methods, which can lead to significant complications when grain sizes are unclear or incomplete. The analyst may not be able to influence these boundaries due to shallow angles or because they are not decorated with small grains. In this case, conventional measurements of the midlines will give overestimates of grain size, as some grains will overlap each other making them appear larger than they actually are [5].

3. IMAGE ANALYSIS AND MEASURING POROSITY

Porosity is the volumetric ratio of pores in a given material. These pores can be found on the surface or in the internal structure of the material. Porosity is related to the density of the material, the nature of its compounds, and the presence of voids between them. High or low porosity can affect the performance of the material. [6].

Total porosity is defined as the fraction of the sample volume V_b that is not occupied by solids. If the solid volume is represented by V_s and the pore volume is represented by $V_p = V_b - V_s$, then the porosity can be expressed as follows [7]:

$$\phi = \frac{V_p}{V_b} = \frac{\text{Pore Volume}}{\text{Total Bulk Volume}} \quad (1)$$

The porosity of thin layers is usually determined using gravimetric or quasi-gravimetric methods [8]. The most obvious and simplest measurement of pore size and pore distribution is the geometric analysis of individual pore images. This can be done using various types of microscopes or using a scanner on a thin section or other flat surface. The dimensions of the pore body and neck can be measured manually or by computer analysis of a digitized image. [7].

3.1 Object Boundary Detection

Polycrystalline films are typically composed of microcrystals interconnected by grain boundaries. The grain boundary regions are disordered, containing a large number of defect states due to incomplete atomic bonds or deviations from the chemical ratios of the semiconductor compound [9]. The evaporation of certain elements changes the chemical ratios and may produce other defects. These changes lead to changes in the film structure and phase of the material, which also affect the electrical, optical and electronic properties. Grain boundary inspection plays an important role in crystal research. After converting the grayscale image to a binary image (by setting a threshold), image processing techniques are used to detect the crystal boundaries using edge detection [10]. The resulting binary image is often full of noise, so a filtering step is necessary to clean up the image for further processing.

3.2 Surface Roughness Analysis

Numerous surface/interface morphologies and film microstructures that are intrinsically linked to dynamic growth mechanisms can be obtained under various film preparation conditions (substrate temperature, pressure, growth rate, presence of impurities, etc.) and growth methods (thermal evaporation deposition, sputtering, chemical vapour deposition, etc.). Physical characteristics are thus significantly and typically differently influenced by them. [11].

Finding a surface's roughness characteristics is the primary task of roughness analysis. Roughness parameters are statistical metrics used to quantify the surface's vertical properties. Determining the roughness parameter, multi-resolution filtering, and picture pre-processing are the three basic steps involved in roughness analysis of 2D color images. The roughness parameters employed in this study are briefly described as follows:

1. The average roughness deviation of all points from a plane to the test part surface is known as the arithmetical mean deviation, or Ra. It may be acquired by [12]:

$$R_a = \frac{1}{n_x n_y} \sum_{i=1}^{n_x} \sum_{j=1}^{n_y} |Z(i, j) - Z_{ave}| \quad (2)$$

Where, $Z(i, j)$ denotes the topography data for the surface, Z_{ave} average surface height, i and j corresponded to the pixels intensities in the x and y direction and n_x and n_y maximum number of pixels in the x and y directions.

2. Root Mean Square (RMS) deviation (R_q): The average of the measured elevation deviations within a length or area assessment, measured from the mean linear surface. It is calculated as follows:

$$R_q = \left[\frac{\sum_{i=1}^{n_x} \sum_{j=1}^{n_y} [Z(i, j) - Z_{ave}]^2}{n_x n_y} \right]^{\frac{1}{2}} \quad (3)$$

Another method used in this study is the number of bright (b) and dark (d) regions. In this method, the number of dark and bright regions in the images is related to the surface texture. The number is the number of objects or pixels in this case in binary images that have the same value 0 or 1, and two pixels are considered part of an object if they are adjacent horizontally, vertically or diagonally.

4 METHODS AND APPLICATIONS

CdTe thin films were deposited using flash evaporation technique on clean glass substrates kept at room temperature. The evaporation process was performed using a vacuum system (Edward 306A) under high vacuum of about 10^{-5} mbar. A molybdenum boat was used as source. They were ultrasonically cleaned with acetone before deposition on the glass substrates. Deionized water and finally dried with a hair dryer. CdTe films with different thicknesses of 400, 500, 600 and 1000 nm were prepared. The thickness of the prepared CdTe films was measured using a profilometer. The CdTe films were annealed at two different temperatures T_a (373 and 473) for 30 min. The surface structure of the deposited films was studied using a scanning electron microscope (SEM). The implementation

of the image processing algorithm aims to provide some important statistical data, where the SEM images of the films were extracted.

4.1.Scanning Electron Microscope (SEM) Analysis:

This section includes the presentation and discussion of the SEM results of CdTe films using Matlab2012. The effect of different thicknesses and annealing processes on the porous surface of these films will be discussed, in addition to the main conclusions drawn.

- **Calculate Porosity Flowchart**

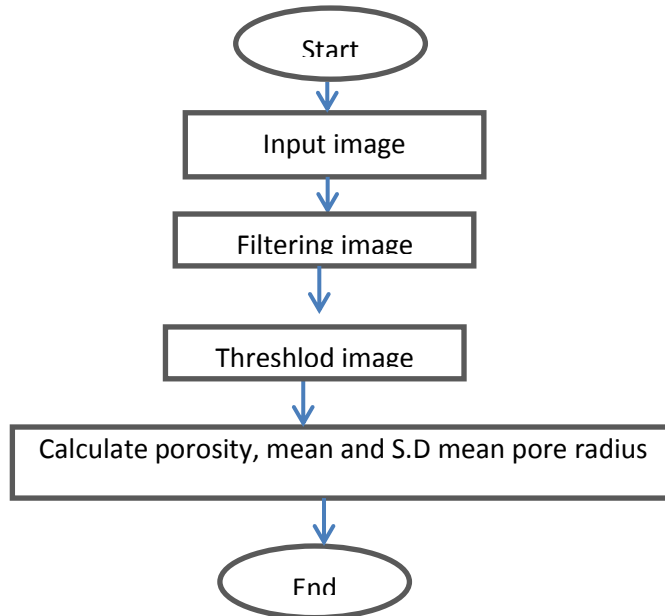


Figure (1): Calculate Porosity Flowchart

- **Grain Boundary Detection Flowchart**

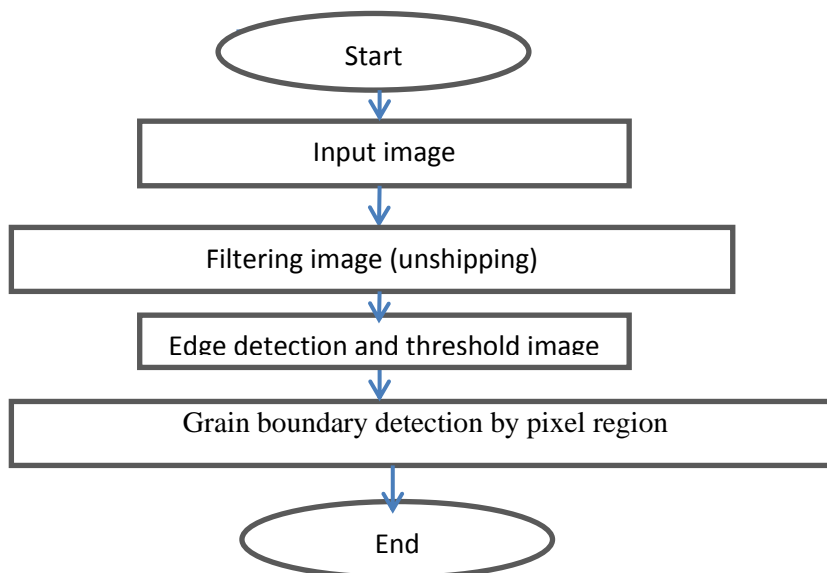


Figure (2): Grain boundary detection flowchart

- **Surface Roughness Flowchart**

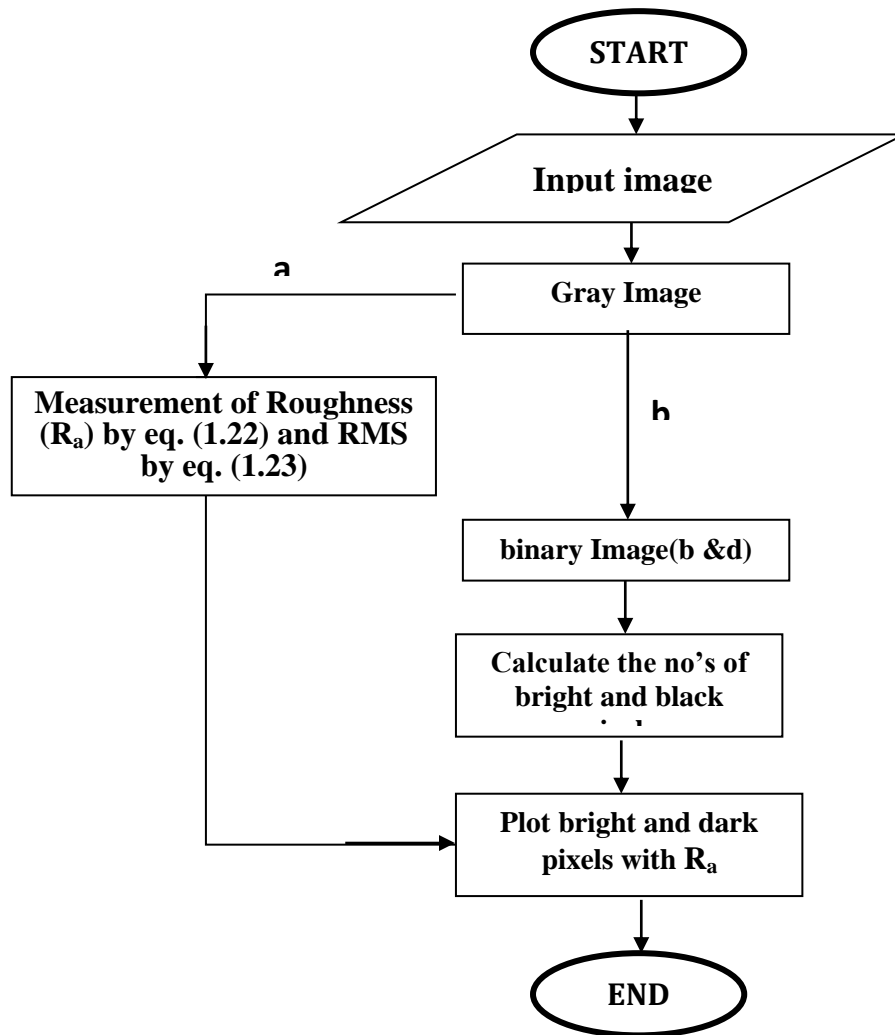


Figure (3): Surface Roughness Flowchart

5 .RESULTS AND DISSOCIATION

5.1 Analysis and Measuring Porosity

Images taken at a specified magnification are used to measure porosity and the distribution of average pore radii in the film.

Figure (4) shows the SEM images pre-treatment operated on CdTe thin film. And table (1) shows, porosity, the mean pore radius of CdTe thin films at different thicknesses, substrate and annealing temperatures.

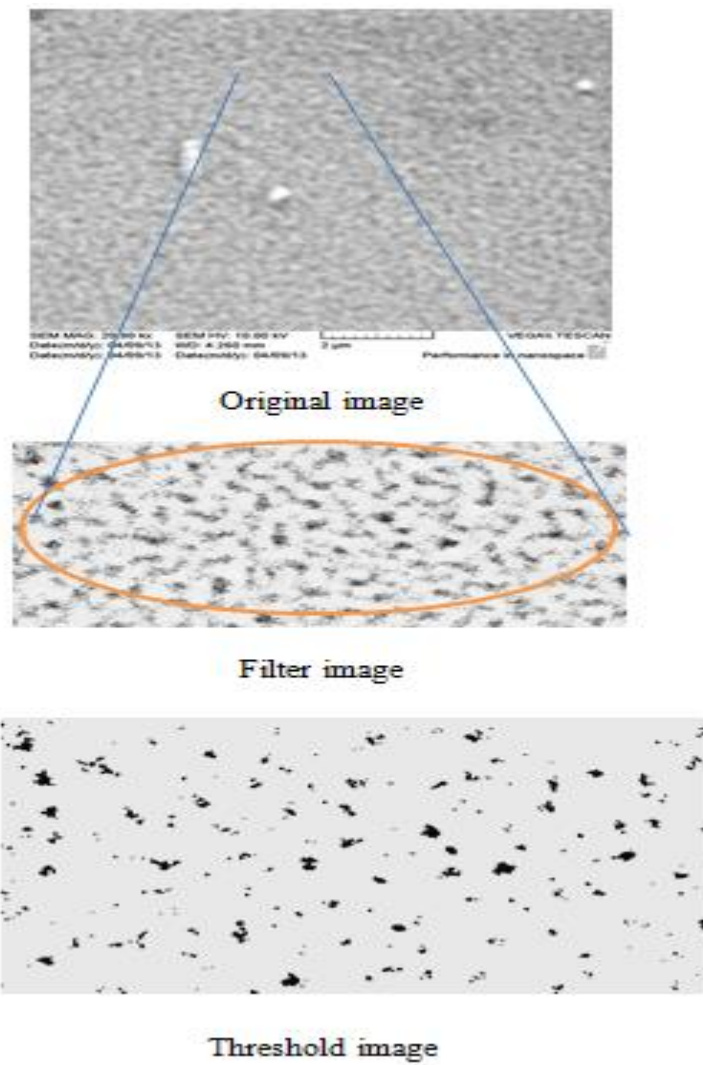


Figure (4): SEM Image pre-treatment operated on CdTe thin film

Table (1): porosity (%), mean and standard deviation for pore radius (nm) of CdTe thin films

t (nm)	Ts (K)	Ta (K)	Porosity (%)	Pore radius(nm)	
				Mean values	Standard deviation
400	303	as deposited	5.6	6.1	2.4
		373	5.2	5.8	2.4
		473	5.0	4.7	2.2
	373	as deposited	5.3	5.8	2.3
		373	5.2	5.2	2.1
		473	4	5	2.0
500	303	as deposited	5.3	5.1	2.0
		373	5.1	4.9	1.9
		473	5.0	4.7	1.9
	373	as deposited	5.15	4.8	1.9
		373	4.8	4.3	1.7
		473	4.6	4.2	1.7
600	303	as deposited	4.8	4.5	1.8
		373	4.6	4.2	1.6
		473	4.5	4.1	1.6
	373	as deposited	4.6	4.3	1.6
		373	4.1	4	1.5
		473	3.9	3.9	1.5
1000	303	as deposited	3.0	3.5	1.3
		373	2.8	3.2	1.2
		473	2.75	3.2	1.2
	373	as deposited	2.8	3	1.2
		373	2.60	2.6	1.1
		473	2.5	2.5	1.1

From table (1) we found that the Porosity decreases with increasing of thickness, substrate and annealing temperature. This behavior can be attributed to the improvement in perfection of the film quality. The mean pore radius values reported in table (1) which shows that, the pore radius falls in the range 2.5-6.1 nm for all investigated films.

5.2 Grain boundary Detection

Figure (5) shows the edge detected image and corresponding pixel region on SEM images of the CdTe thin film. After filtering the image those images are subjected to edge detected image shows the pixel regions of the grain boundary thin film as ones.

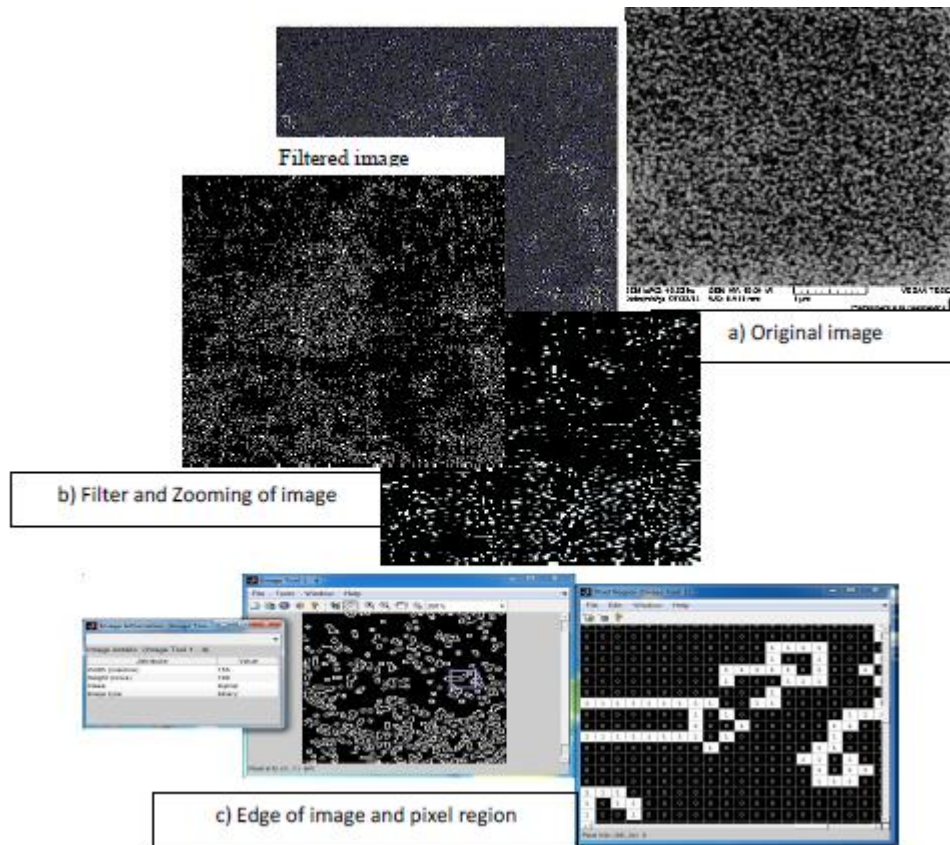


Figure (5): shows applied the grain boundary detection on SEM images of CdTe thin film

After applying this technique on SEM image of CdTe thin films for different thicknesses, substrate and annealing temperatures, we can find from table (2) that the grain boundary decrease with increasing thickness, substrate and annealing temperature. These results are attributed by increasing the thickness and substrate , annealing temperature the grain size increases, which leads to decrease grain boundaries volume. This is in agreement with V. Krishnakumar et al. [13].

Table (2): The grain boundary (nm) of CdTe thin films

(nm)	T _s (K)	T _a (K)	Grain boundary (nm)
400	303	as deposited	135-389
		373	134 -300
		473	120-278
	373	as deposited	130- 366
		373	127-280
		473	118-260
500	303	as deposited	110-260
		373	108-200
		473	100-188
	373	as deposited	109-220
		373	103-170
		473	99- 160
600	303	as deposited	102 –189
		373	98-150
		473	97-140
	373	as deposited	99-176
		373	92-160
		473	88-155
1000	303	as deposited	80-160
		373	77-150
		473	72-148
	373	as deposited	79 -155
		373	75-167
		473	78- 130

5.3 Measurement of Surface Roughness

After applying stage algorithm of surface roughness (figure(3)) by using equations (2) and (3) on SEM image of CdTe thin films for different thicknesses, substrate and annealing temperatures, we can find from table (3) , the surface roughness (R_a) and RMS surface roughness of the CdTe film increases with the increase in film thickness , substrate and annealing temperatures. similar result have been observe by Patel at el.[14] by using atomic force microscopy technique (AFM).

Table (3): The value of average roughness, RMS and average grain size for CdTe thin films

t (nm)	Ts (K)	Ta (K)	Average Roughness (R_a)(nm)	RMS (nm)
400	303	as deposited	0.29	0.41
		373	0.36	0.50
		473	0.50	0.59
	373	as deposited	0.49	0.47
		373	0.56	0.62
		473	0.70	0.89
500	303	as deposited	0.53	0.50
		373	0.62	0.75
		473	0.74	0.86
	373	as deposited	0.59	0.62
		373	0.83	0.73
		473	0.92	1.07
600	303	as deposited	1.05	1.29
		373	1.15	1.44
		473	1.48	1.87
	373	as deposited	1.12	0.25
		373	1.28	1.71
		473	1.54	1.95
1000	303	as deposited	1.55	2.01
		373	1.81	2.25
		473	2.13	2.69
	373	as deposited	1.79	2.18
		373	1.92	2.69
		473	2.28	2.90

Figure (6) shows the stages effect of bright (b) and dark (d) region counts described in figure (3) application on SEM Images of CdTe thin films.

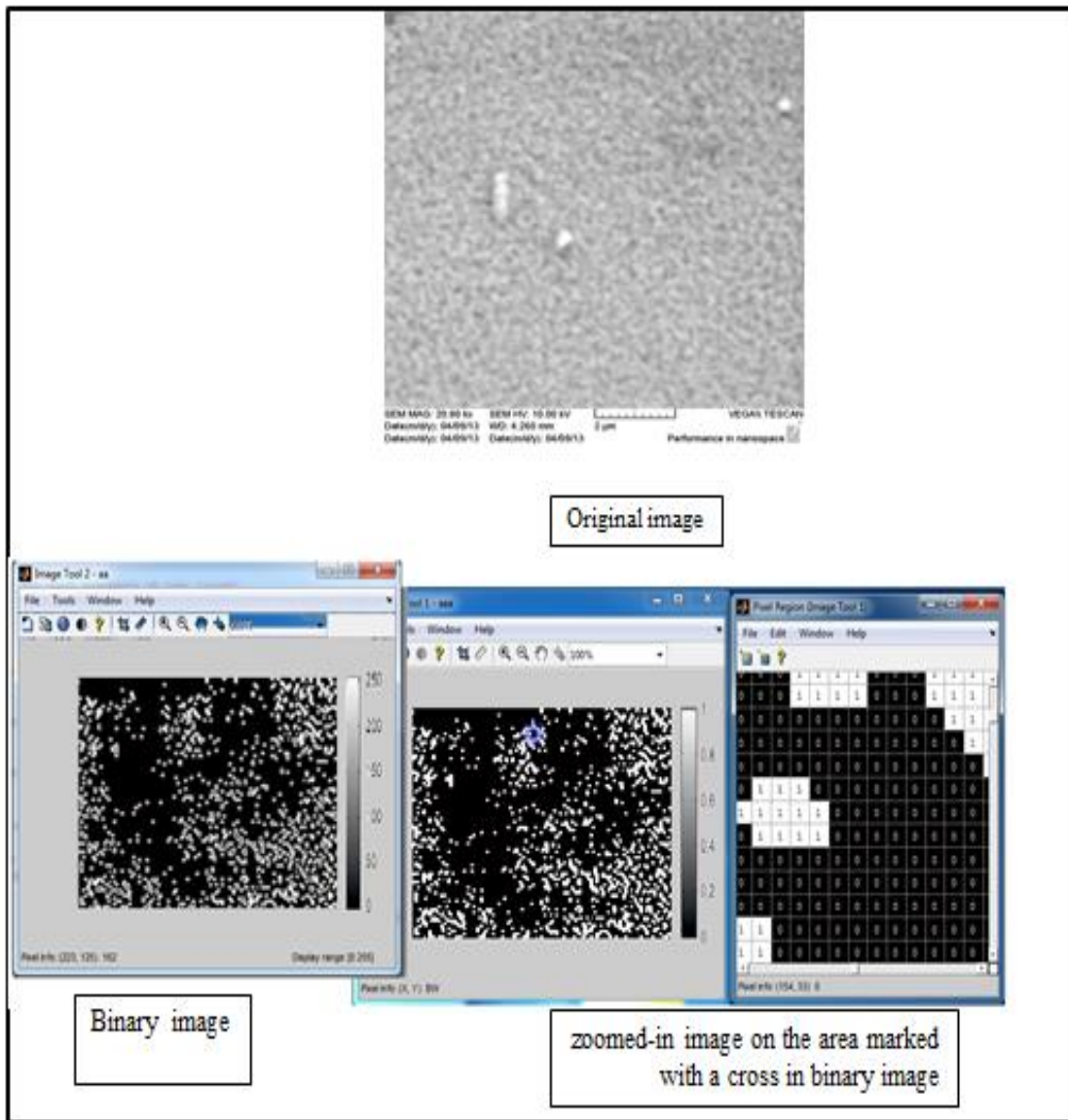


Figure (6): shows applied the effect of B and D region counts on SEM images of CdTe thin film

Figure (7) shows the variation of Ra values of SEM images of CdTe thin film, with the values of the number of dark and bright regions calculated from the binary images. It can be seen from Figure (7) that the number of dark and bright regions increases linearly with increasing surface roughness. Therefore, the number of bright and dark regions can be used as a practical method to determine the surface roughness.

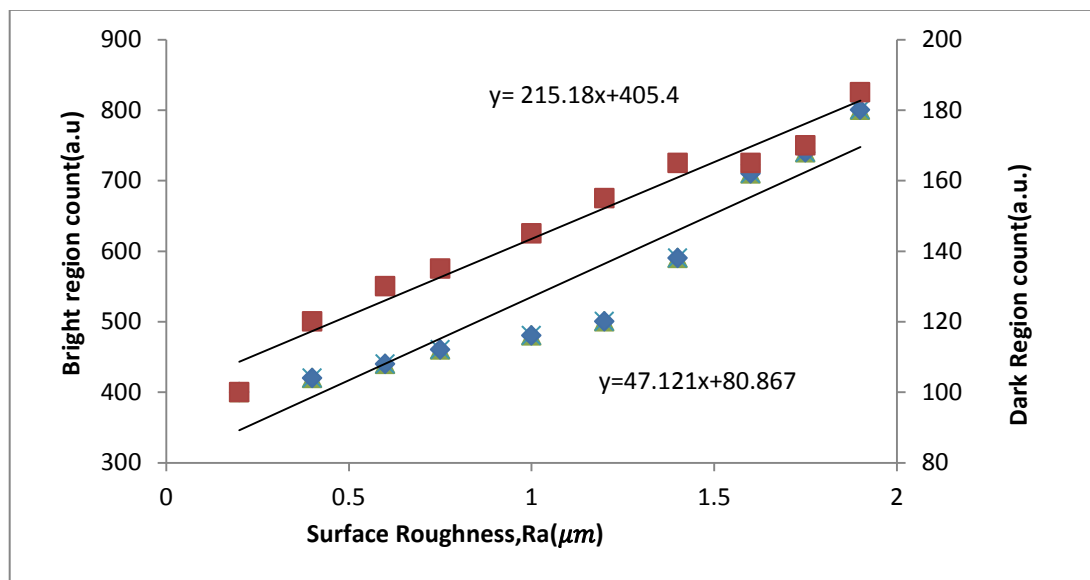


Figure (7): Variation of bright and dark region counts with Ra Values for SEM images for CdTe thin films

CONCLUSION

Digital image processing techniques are used to study the structure properties of CdTe films. This technique offers the advantages of greater accuracy and the ability to determine individual components of the microstructure,

ACKNOWLEDGMENTS

The author would like to thank Mustansiriyah University (<https://www.uomustansiriyah.edu.iq/>), Baghdad –Iraq for its support in the present work.

REFERENCES

- [1] S. H. Ibraheem, I. M. Abdulmajeed. "The effect of metal Ag nanoparticles on CdS/ZnTe heterojunction solar cells", Chalcogenide Letters Vol. 20, No. 9, September, p. 677 – 683, (2023).
<https://doi.org/10.15251/CL.2023.209.677>
- [2] Rakhshani A, "Electrodeposited CdTe - optical properties", J. Appl. Lett., 81, p. 7988–7993 (1997).
- [3] Ziad M. Abood, Raad M. S. Al-Haddad & Suha H. Ibraheem, "The Study of properties of AFM image of CdTe thin films using FCM and Marker-Controlled Watershed Segmentation", International Journal for Sciences and Technology / ICV: 4.32 Vol. 9, No.1, March 2014
<https://platform.almanhal.com/Reader/Article/60445>.
- [4] Manuel F. M. Costa "Image processing. Application to the characterization of thin films" Journal of Physics: Conference Series 274 (2011) 012053
- [5] Ian T. Young, Jan J. Gerbrands, and Lucas J. van Vliet, "Fundamentals of Image Processing". Delft University of Technology, (1995).
- [6] Lawrence M. Anovitz, David R. Cole; Characterization and Analysis of Porosity and Pore Structures. Reviews in Mineralogy and Geochemistry 2015;; 80 (1): p.61–164.
doi: <https://doi.org/10.2138/rmg.2015.80.04>
- [7] Nimmo. J. R., "Porosity and Pore Size Distribution", in Hillel, D., ed. Encyclopedia of Soils in the Environment: London, Elsevier 3, p.295-303, (2004).
- [8] S. Nakahara, "Porosity in Thin Films". Thin Solid Films, 64, 149 (1979).
- [9] P. Meakin, Fractals, "Scaling, and Growth Far from Equilibrium" (Cambridge University Press, Cambridge, (1998)
- [10] S. Zheng, Z. Tu and A. L. Yuille, "Detecting Object Boundaries Using Low-, Mid-

- , and High-level Information," 2007 IEEE Conference on Computer Vision and Pattern Recognition, Minneapolis, MN, USA, 2007, pp. 1-8, doi: 10.1109/CVPR.2007.383343.
- [11] P. Meakin, Fractals, "Scaling, and Growth Far from Equilibrium"(Cambridge University Press, Cambridge, (1998)
- [12] S. Ondimu, H Murase," Image Processing and Roughness Analysis as a Tool for Quantification of Physiological Well-Being in plants": Results for Sunagoke Moss, IFAC World Congress, 17, p.641- 646, (2008).
- [13] V. Krishnakumar, J. Han, A. Klein, W. Jaegermann,CdTe thin film solar cells with reduced CdS film thickness, Thin Solid Films,Volume 519, Issue 21,(2011),
- [14] H. S. Patel, J. R. Rathod, K. D. Pateland and V. M. Pathak " Structural and Surface Studies of Vacuum Evaporated Cadmium Telluride Thin Films", American Journal of Materials Science andTechnology,1,pp.11- 21, (2012).

Email: dr.suhad@uomustansiriyah.edu.iq